J Ind Microbiol Biotechnol (2011) 38:51–64
DOI 10.1007/s10295-010-0828-0

ORIGINAL PAPER

Nickel(II) biosorption by *Rhodotorula glutinis*

Alicia Suazo-Madrid · Liliana Morales-Barrera · Erick Aranda-García · Eliseo Cristiani-Urbina

Received: 25 March 2010 / Accepted: 26 July 2010 / Published online: 5 September 2010

Abstract The present study reports the feasibility of using *Rhodotorula glutinis* biomass as an alternative low-cost biosorbent to remove Ni(II) ions from aqueous solutions. Acetone-pretreated *R. glutinis* cells showed higher Ni(II) biosorption capacity than untreated cells at pH values ranging from 3 to 7.5, with an optimum pH of 7.5. The effects of other relevant environmental parameters, such as initial Ni(II) concentration, shaking contact time and temperature, on Ni(II) biosorption onto acetone-pretreated *R. glutinis* were evaluated. Significant enhancement of Ni(II) biosorption capacity was observed by increasing initial metal concentration and temperature. Kinetic studies showed that the kinetic data were best described by a pseudo-second-order kinetic model. Among the two-, three-, and four-parameter isotherm models tested, the Fritz-Schluender model exhibited the best fit to experimental data. Thermodynamic parameters (activation energy, and changes in activation enthalpy, activation entropy, and free energy of activation) revealed that the biosorption of Ni(II) ions onto acetone-pretreated *R. glutinis* biomass is an endothermic and non-spontaneous process, involving chemical sorption with weak interactions between the biosorbent and Ni(II) ions. The high sorption capacity (44.45 mg g^{-1} at 25°C, and 63.53 mg g^{-1} at 70°C) exhibited by acetone-pretreated *R. glutinis* biomass places this biosorbent among the best adsorbents currently available for removal of Ni(II) ions from aqueous effluents.

Keywords Isotherm · Kinetics · Nickel(II) biosorption · *Rhodotorula glutinis* · Thermodynamics

This article is part of the BioMicroWorld 2009 Special Issue.

A. Suazo-Madrid · L. Morales-Barrera · E. Aranda-García · E. Cristiani-Urbina (✉)
Departamento de Ingeniería Bioquímica,
Escuela Nacional de Ciencias Biológicas,
Instituto Politécnico Nacional,
Prolongación de Carpio y Plan de Ayala s/n,
Colonia Santo Tomás, Mexico, DF 11340, Mexico
e-mail: ecristia@encb.ipn.mx

Introduction

Divalent nickel [Ni(II)] is a toxic heavy metal present in raw wastewater streams from industries such as electroplating, non-ferrous metal, mineral processing, paint formulation, porcelain enameling, copper sulfate and battery manufacture, as well as from steam-electric power plants [1]. The effluent emanating from these industries often contains high concentrations of Ni(II) ions, which are toxic to both higher and lower organisms [1, 2]. In humans, Ni(II) can cause various types of acute and chronic health disorders, such as severe damage of lungs and kidney, skin dermatitis, nausea, vomiting, diarrhea, pulmonary fibrosis, renal edema, chest pain, rapid respiration, cyanosis and extreme weakness [3, 4]. Besides, it is well known that nickel is carcinogenic and this effect is probably related to its lipid-peroxidation properties, which induce DNA-strand gaps and breaks, and DNA–protein crosslinks [5]. Moreover, nickel has been implicated as a nephrotoxin [5], teratogen and embryotoxin [3].

The United States Environmental Protection Agency (EPA) and the World Health Organization (WHO) have established drinking water guidelines for nickel of 0.1 mg l^{-1} [6] and 0.07 mg l^{-1} [7], respectively. In order to meet the water quality standards for most countries, it is essential to reduce the concentration of Ni(II) ions and of other heavy metals in industrial wastewaters to their permissible limits before discharge to the environment.

A number of conventional technologies, such as adsorption on activated carbon, ion exchange, chemical precipitation and crystallization in the form of nickel carbonate, have been used to remove Ni(II) ions from industrial wastewaters, surface water and ground waters [6, 7]. However, these technologies are either ineffective or expensive when heavy metals are present in the waters at low concentrations, usually in the range of 1–100 mg l^{-1}, or when low concentrations of heavy metals in treated waters are required [8]. Therefore, it is crucial to develop economic, efficient and secure technologies to remove heavy metals in order to protect the environment, and public health and safety in a cost effective and environmentally friendly manner.

Biosorption has emerged as an alternative sustainable strategy for cleaning up water that has been contaminated with toxic metals by anthropogenic activities and/or by natural processes [9]. It utilizes the properties of certain kinds of inactive or dead biomass to bind and accumulate these pollutants by different mechanisms, such as physical adsorption, chemisorption, complexation, ion exchange and surface-microprecipitation [10]. A vast array of biological materials, especially bacteria, algae, yeasts and filamentous fungi have received increasing attention due to their good performance regarding heavy metal removal and water recovery, as well as their low cost and large available quantities [11].

Despite the well-known potential of yeasts to remove heavy metal cations from aqueous solutions, only scarce information is available on the sorption ability of heavy metals by *Rhodotorula glutinis* [12, 13]. This yeast is distributed widely in nature and is potentially useful to industry since it is able to produce carotenoids when grown on various cheap raw materials of agro-industrial origin [14, 15]. The biomass left after carotenoid extraction from *R. glutinis* is a waste material from biotechnological processes that may be used as a potential biosorbent for the removal of heavy metals from aqueous solutions.

To the best of our knowledge, *R. glutinis* has not been used previously as a biosorbent for Ni(II) biosorption from aqueous solutions containing this heavy metal. In *Saccharomyces cerevisae*, a yeast amply studied for biosorption purposes, the highest Ni(II) biosorption level was at pH 5 [16]. In the case of protonated baker's yeast and of three different species of *Candida*, the highest Ni(II) biosorption levels were obtained at pH values of 6.75 [2] and 6.5 [17], respectively.

The main aim of the present work was to study the effect of different environmental parameters such as pH, initial Ni(II) concentration, contact time, and temperature on the ability of untreated and acetone-pretreated *R. glutinis* biomass to biosorb Ni(II) ions from aqueous solutions. Furthermore, the kinetics, isotherm and thermodynamics of Ni(II) biosorption by *R. glutinis* are described.

Materials and methods

Microorganism

The *Rhodotorula glutinis* strain used throughout this work was obtained from the Biotechnology and Bioengineering Department Culture Collection at the Centro de Investigación y de Estudios Avanzados (CINVESTAV), Instituto Politécnico Nacional, Mexico. The yeast was maintained on YPD agar slants (2% dextrose, 1% yeast extract, 1% casein peptone, and 2% agar) at 4°C.

Preparation of *R. glutinis* biomass for biosorption experiments

Rhodotorula glutinis yeast cells were grown in 500 ml Erlenmeyer flasks containing 100 ml liquid YPD medium (20 g l^{-1} dextrose, 10 g l^{-1} yeast extract, and 10 g l^{-1} casein peptone). Yeast cultures were incubated in a shaker (model K12504-70, Cole Parmer, Vernon Hills, IL) at 120 rpm for 24 h at 25°C. The yeast cells obtained were separated by centrifuging at 3,500 rpm for 15 min, and washed three times with distilled deionized water. The resulting cell pellet was then divided into two equal portions. One portion was dried at 60°C for 24 h and used further for Ni(II) biosorption experiments. The other portion was treated three times with analytical grade acetone (Baker, Phillipsburg, NJ), following the procedures described by Aksu and Eren [14], in order to extract total carotenoids. The acetone-pretreated yeast biomass was then washed thoroughly with distilled deionized water, dried at 60°C for 24 h, and subsequently used for Ni(II) biosorption experiments.

Nickel(II) solutions for biosorption experiments

Ni(II) solutions were obtained by diluting 2 g l^{-1} stock Ni(II) solution, which was prepared by dissolving a weighed quantity of analytical grade nickel sulfate hexahydrate ($NiSO_4 \cdot 6H_2O$; Baker, purity >99.1%) in distilled deionized water. In this work, the initial Ni(II) concentration varied from 10 to 400 mg l^{-1} and the pH of each Ni(II) solution was adjusted to desired pH value in the range of 3–7.5 ± 0.1 with 0.1 *N* HCl and NaOH solutions.

Batch biosorption studies and analytical method

Batch biosorption dynamics were analyzed to determine the effect of solution pH, initial Ni(II) concentration, shaking contact time and temperature on Ni(II) biosorption by *R. glutinis* biomass. All experiments were conducted in 500 ml Erlenmeyer flasks containing 100 ml Ni(II) solution of known concentration and 1 g (dry weight) l^{-1} yeast

biomass. The pH of each Ni(II) solution was maintained constant (±0.1 pH unit) throughout the course of the experiments by periodic checking and adjustment with 0.1 *N* HCl and/or NaOH aqueous solutions. Flasks were agitated in a shaker (model K12504-70, Cole Parmer) at 140 rpm constant shaking speed.

Untreated biomass and acetone-pretreated biomass of *R. glutinis* were used as biosorbents to study the influence of pH level on Ni(II) sorption. These experiments were performed at different pH values ranging from 3 to 7.5 ± 0.1, with a Ni(II) solution at an initial metal concentration of 60 mg l^{-1} [approximately 1 mM Ni(II)], at 25°C. In these experiments, the acetone-pretreated biomass of *R. glutinis* exhibited higher Ni(II) ion biosorption capacity than the untreated biomass, so that the acetone-pretreated biomass was chosen for subsequent studies. In addition, the optimum pH value for Ni(II) biosorption by acetone-pretreated biomass was determined to be 7.5 and used thereafter.

The effect of contact time on Ni(II) biosorption of between 0 and 120 h was studied, with Ni(II) solutions at initial metal concentrations ranging from 10 to 400 mg l^{-1}, at 25°C.

To investigate the effect of initial Ni(II) concentration on kinetic performance, experiments were carried out with Ni(II) solutions at initial metal concentrations ranging from 10 to 400 mg l^{-1}, at 25°C.

For the isotherm studies, the biosorbent (1 g l^{-1}) was brought into contact with solutions of different initial Ni(II) concentration (10–400 mg l^{-1}) at 25°C, with constant agitation (140 rpm) for 120 h to ensure sorption equilibrium was reached.

The effect of temperature on Ni(II) biosorption was studied by varying temperatures from 25 to 70°C and two different initial Ni(II) concentrations (60 and 150 mg l^{-1}) were used.

Blanks and biosorbent-free controls were run concurrently and under exactly the same conditions as those used for the Ni(II) biosorption experiments in order to check for glassware sorption of the heavy metal and other side potential effects (metal precipitation, etc.). Biosorbent-free controls included Ni(II) solutions but not biosorbent, and blanks consisted on biosorbent and distilled deionized water. No measurable change in Ni(II) concentration was detected in the blanks and biosorbent-free controls throughout the various sorption experiments conducted in our work, which suggests that the observed removal of Ni(II) in the experiments with *R. glutinis* biomass was due only to the biosorbent.

Samples were collected at different experimental times and filtered through 1.6 μm filters (Whatman GF/A). The filtrates obtained were then analyzed for Ni(II) concentrations by using the dimethylglyoxime method [18]. The absorbance of the wine red-to-brown colored complex of Ni(II) ion with dimethylglyoxime was read at a wavelength of 465 nm in a Genesys™ 10 UV–Visible spectrophotometer (Thermo Scientific, Rockford, IL).

The amount of Ni(II) sorbed at time *t* by the biosorbent (q_t), which represents the Ni(II) biosorption capacity (mg g^{-1}), was calculated according to the following mass balance relationship:

$$q_t = \frac{c_o - c_{res}}{X} \quad (1)$$

where C_o is initial Ni(II) concentration (mg l^{-1}) at time $t_o = 0$ h, C_{res} is residual Ni(II) concentration (mg l^{-1}) at time $t = t$, and X is biosorbent concentration (g l^{-1}). At the sorption equilibrium, C_{res} equals the equilibrium concentration of Ni(II) ions in the solution (C_e, mg l^{-1}) and q_t equals Ni(II) sorption uptake or equilibrium biosorption capacity of Ni(II) (q_e, mg g^{-1}).

Batch experiments were conducted in triplicate and the mean values are reported herein. The maximum coefficient of variation of the three replicas was 5%.

Ni(II) biosorption data were analyzed statistically by analysis of variance (Holm-Sidak method; overall confidence level = 0.05) using SigmaStat 3.5 software. Statistical analysis revealed that the longest contact time required to reach the sorption equilibrium was 2 h and this was found when high initial Ni(II) concentrations were tested; therefore, the results obtained during the first 4 h of contact only are shown in the present work.

Biosorption kinetics modeling

In order to evaluate the kinetic mechanism that controls the Ni(II) biosorption process, pseudo-first-order and pseudo-second-order kinetic models were tested to interpret the experimental data [6, 19]. The pseudo-first-order model and pseudo-second-order model parameters were evaluated by non-linear regression analysis using MATLAB® software (version 7.9; http://www.mathworks.com/products/matlab).

Equilibrium modeling

The equilibrium distribution of Ni(II) ions between the liquid phase and *R. glutinis* biomass was expressed in terms of a Ni(II) biosorption isotherm. Several two-parameter (Langmuir, Freundlich, Temkin and Dubinin-Radushkevich) [6, 16, 20], three-parameter (Sips, Toth, Redlich-Peterson and Radke-Prausnitz) [20–22], and four-parameter (Fritz-Schluender) [23] sorption isotherm models were used to fit the experimental equilibrium data obtained at different initial Ni(II) concentrations.

Thermodynamic studies

From the results obtained in the kinetic study carried out at different temperatures, the activation energy (E_A) for Ni(II) biosorption was calculated by the Arrhenius equation:

$$k_2 = A_0 \exp^{\left(\frac{-E_A}{RT}\right)} \quad (2)$$

Taking the natural log of both sides of Eq. 2, one obtains:

$$\ln k_2 = \ln A_0 - \frac{E_A}{RT} \quad (3)$$

where k_2 is the rate constant of second-order biosorption (g mg^{-1} h^{-1}), A_0 (g mg^{-1} h^{-1}) is the frequency factor [24], and E_A is the activation energy (kJ mol^{-1}). By plotting ln k_2 versus T^{-1}, a linear relationship is obtained and one can determine E_A from the slope ($-E_A/R$) and A_o from the y-intercept.

In environmental engineering practice, both energy and entropy factors must be considered in order to determine whether a process will occur spontaneously or not. Therefore, in the present work, the changes in enthalpy ($\Delta H^{\ddagger}$), entropy ($\Delta S^{\ddagger}$) and Gibbs free energy ($\Delta G^{\ddagger}$) of activation for Ni(II) biosorption were calculated by the Eyring equation [25]:

$$\ln \frac{k_2}{T} = \ln \frac{k_b}{h} + \frac{\Delta S^{\ddagger}}{R} - \frac{\Delta H^{\ddagger}}{RT} \quad (4)$$

where k_b is the Boltzmann constant (1.3807×10^{-23} J K^{-1}) and h is the Planck constant (6.6261×10^{-34} J s).

The Gibbs free energy change of activation ($\Delta G^{\ddagger}$) may be described in terms of entropy change and enthalpy change of activation, as follows [25]:

$$\Delta G^{\ddagger} = \Delta H^{\ddagger} - T\,\Delta S^{\ddagger} \quad (5)$$

Non-linear regression analysis

All the model parameters were evaluated by non-linear regression using MATLAB® software (version 7.9). The optimization procedure requires an error function to be defined in order to be able to evaluate the fit of the mathematical model to the experimental data [26]. Therefore, the correlation coefficient (r^2), the residual or sum of squares error (SSE), the root mean squared error or standard error (RMSE) of the estimate and the 95% confidence intervals of the models parameters were used with the purpose of measuring the goodness-of-fit of the sorption models.

SSE can be defined as [26]:

$$SSE = \sum_{i=1}^{m} (Qi - qi)^2 \quad (6)$$

RMSE can be defined as follows [26]:

$$RMSE = \sqrt{\frac{1}{m-p}\sum_{i=1}^{m} (Qi - qi)^2} \quad (7)$$

where q_i is the experimental sorption capacity from the batch experiment i, Q_i is the sorption capacity estimated from the sorption model for corresponding q_i, m is the number of observations in the batch experiment and p is the number of parameters in the regression model [26]. The closer r^2 to 1.0 and the smaller SSE, RMSE and confidence interval values indicate the better curve fitting.

Results and discussion

Effect of pH on Ni(II) ion biosorption

The present work analyzed the effect of solution pH on Ni(II) biosorption onto *R. glutinis* biomass, either untreated or pretreated with acetone to extract total carotenoids. Different pH levels were assayed within the range of 3 to 7.5 ± 0.1, which were kept constant along each experiment. It is known that at pH > 7.7, hydroxide ions (OH^-) in solution may bind to Ni(II) ions to form hydroxylated nickel complexes, such as nickel hydroxide, which tend to precipitate in solution [27, 28]. Under these pH conditions a combined process of nickel biosorption and microprecipitation occurs in which the latter predominates.

In the present study, it was found that, at the different pH levels tested, the Ni(II) biosorption capacity of untreated and acetone-pretreated *R. glutinis* increased as contact time increased, until it reached a maximum constant value, which corresponded to biosorption equilibrium (Fig. 1). Furthermore, Ni(II) biosorption onto the untreated or acetone-pretreated *R. glutinis* biomass depended strongly on solution pH. Ni(II) biosorption capacity increased as pH levels rose and was highest at pH 7.5, both for untreated and for acetone-pretreated yeast (Fig. 1).

The low levels of Ni(II) biosorption capacity observed at low pH levels could be attributed to the high concentration of hydrogen (H^+) and hydronium (H_3O^+) ions in solution, which compete with Ni(II) ions for the binding sites present in the biomass. At low pH levels, the concentration of H^+ and H_3O^+ ions greatly exceeds the Ni(II) ion concentration and, therefore, the former bind to the ligands and leave Ni(II) ions unbound [29]. As the pH increases, the competing effect of the H^+ and H_3O^+ ions diminishes and the positively charged Ni(II) ions are adsorbed to the free binding sites [2].

The effect of pH on Ni(II) biosorption may also be explained by the ionization of cell surface ligands, which

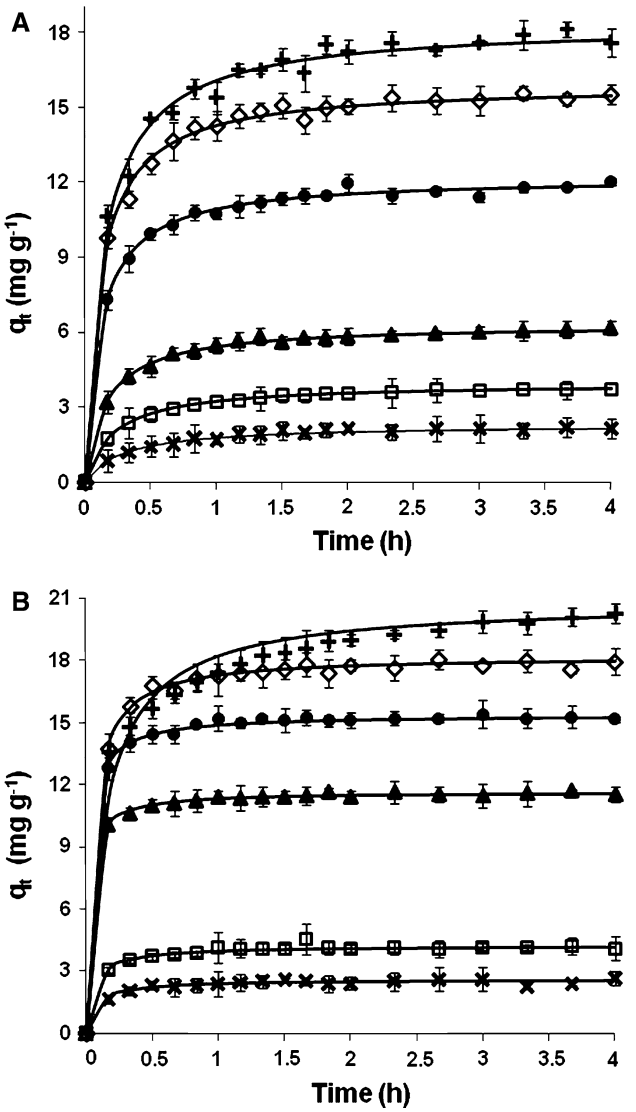

Fig. 1 Effect of solution pH on Ni(II) biosorption by untreated (**a**) and acetone-pretreated (**b**) *Rhodotorula glutinis* biomass [solution pH: *multisymbol* 3.0, *open square* 4.0; *filled triangle* 5.0; *filled circle* 6.0; *open diamond* 7.0; *plus symbol* 7.5; *solid line* pseudo-second-order model prediction]. Conditions: initial Ni(II) concentration = 60 mg l^{-1}; temperature = 25°C; biosorbent concentration = 1 g l^{-1}. When not shown, *error bars* are smaller than symbol size

serve as metal binding sites. At high pH values, a net negative charge is present on the cell surface, and the ionic state of the ligands like carboxyl, phosphate, sulfhydril, hydroxyl, imidazole and amino groups is such that it favors the reaction with cationic metals. It is well known that at pH values from 4 to approximately 7.5, Ni(II) ions in aqueous solution are present as divalent positive ions that can interact with negatively charged groups in the biomass [16, 28]. However, as the pH falls, the overall charge of the cell surface becomes more positive, and positively charged cationic metals cannot therefore approach the surface [16, 29].

The highest values of Ni(II) biosorption capacity of untreated and acetone-pretreated *R. glutinis* cells were 18.1 and 21.1 mg g^{-1}, respectively, and these values were obtained at a pH level of 7.5 (Fig. 1). At this optimum pH value, the Ni(II) biosorption capacity of acetone-pretreated *R. glutinis* was 16.6% higher than that of untreated biomass, and this difference was statistically significant ($P < 0.05$). Moreover, at pH 7.5, no statistically significant difference was observed in the biosorption capacities obtained at contact times higher than 1.5 h ($P > 0.05$), which indicates that biosorption equilibrium was reached at this contact time.

As these results show, acetone pretreatment of *R. glutinis* increased the Ni(II) biosorption capacity. This could be because acetone caused a change in cell permeability and removed some organic compounds from the cell wall, which caused an increment in binding site availability and in the access of Ni(II) ions to those sites [30]. These findings are of interest because the *R. glutinis* biomass that remains after total carotenoid extraction with acetone [14, 15] is a waste material with adequate Ni(II) biosorption characteristics, which could be used to detoxify waters contaminated with the metal.

On the other hand, in order to determine the mechanism of Ni(II) biosorption onto *R. glutinis*, pseudo-first-order and pseudo-second-order kinetic models were used to assay experimental data. Table 1 shows the rate constants (k_1 and k_2) and the Ni(II) biosorption capacity in equilibrium (q_e) determined with the models, together with the corresponding correlation coefficients (r^2), SSE and RMSE. As shown, for untreated and acetone-pretreated biomass at all pH levels assayed, with the pseudo-second-order model the correlation coefficients were higher and the SSE and RMSE values lower than those obtained with the pseudo-first-order model. Besides, the values of biosorption capacity at equilibrium (q_e) calculated from the pseudo-second-order model were closer to experimental values (exp q_e) at all assayed pH levels. Furthermore, the pseudo-second-order model described well the variation of Ni(II) biosorption capacity at all contact times and assayed pH levels (continuous lines in Fig. 1). According to these results, the biosorption system of Ni(II) ions using untreated and acetone-pretreated *R. glutinis* biomass followed the pseudo-second-order kinetic model, which suggests that the rate-limiting step was a chemical sorption process involving valence forces through the sharing or exchange of electrons between *R. glutinis* biomass and Ni(II) ions, complexation, coordination and/or chelation [8, 20, 31].

The pseudo-second-order kinetic model has also been applied successfully to Ni(II) biosorption by protonated-baker's yeast [2], *Chlorella vulgaris* [32] as well as by diverse agroindustrial by-products, such as wheat straw [33], hazelnut and almond shells [31], and protonated rice bran [8].

Table 1 Kinetic model parameters for Ni(II) biosorption onto untreated and acetone-pretreated *Rhodotorula glutinis* biomass at different solution pH values

pH	Exp q_e (mg g^{-1})	Pseudo-first-order model					Pseudo-second-order model				
		q_e (mg g^{-1})	k_1 (h^{-1})	r^2	SSE	RMSE	q_e (mg g^{-1})	k_2 (g mg^{-1} h^{-1})	r^2	SSE	RMSE
Untreated biomass											
3	2.309	2.161	2.007	0.9545	0.3199	0.1109	2.32	1.46	0.9803	0.1384	0.0730
4	3.926	3.693	2.632	0.957	0.7902	0.1743	3.937	1.149	0.9978	0.03984	0.0391
5	6.263	5.999	3.365	0.9663	1.5	0.2402	6.33	0.9685	0.9973	0.1193	0.0678
6	12.156	11.660	4.545	0.964	5.561	0.4625	12.19	0.711	0.9968	0.4881	0.137
7	15.860	15.240	4.493	0.9663	8.830	0.5828	15.9	0.555	0.9962	1.000	0.1961
7.5	18.137	17.440	3.829	0.9481	18.74	0.849	18.32	0.3922	0.9891	3.95	0.3898
Acetone-pretreated biomass											
3	2.520	2.489	5.616	0.914	0.6214	0.1490	2.571	4.639	0.9262	0.5334	0.138
4	4.204	4.110	6.93	0.9769	0.4067	0.1205	4.223	3.714	0.9943	0.0999	0.0597
5	11.621	11.490	11.73	0.9895	1.364	0.2207	11.65	3.066	0.997	0.297	0.103
6	15.385	15.150	10.42	0.9914	1.944	0.2635	15.39	1.998	0.9978	0.4918	0.1325
7	18.182	17.770	8.048	0.9797	6.545	0.4835	18.2	1.038	0.9948	1.668	0.2441
7.5	21.143	19.790	4.109	0.8825	55.80	1.4120	20.94	0.3243	0.9723	13.54	0.6832

Conditions: initial Ni(II) concentration, 60 mg l^{-1}; temperature, 25°C; shaking speed, 140 rpm; biosorbent concentration, 1 g l^{-1}. *SSE* Sum of squares error, *RMSE* root mean square error

The present work revealed that the effect of pH on the rate constant (k_2) of the pseudo-second-order model was opposed to the effect of pH on experimental q_e; i.e., the higher the pH level, the lower the k_2 (Table 1). This behavior could be explained because, at pH levels close to neutral, *R. glutinis* cells biosorb larger amounts of Ni(II) ions and therefore require longer periods of contact to reach equilibrium, as shown in Fig. 1. In contrast, at low pH levels, the amount of Ni(II) biosorbed by the yeast is very low, and therefore equilibrium is reached rapidly, which is manifested as a high k_2 value [34, 35].

Optimal characteristics of Ni(II) biosorption onto acetone-pretreated *R. glutinis* cells were found for aqueous solution at pH 7.5, and these conditions were therefore used in subsequent studies. In addition, the pseudo-second-order model was used henceforth to describe Ni(II) biosorption kinetics, since it clearly proved to represent them adequately.

Effect of initial Ni(II) concentration and contact time on metal biosorption

In the present work, the effect of initial Ni(II) concentration and contact time on Ni(II) biosorption onto acetone-pretreated *R. glutinis* was investigated at different initial Ni(II) concentrations, ranging from 10 to 400 mg l^{-1}. Figure 2 shows variations in Ni(II) biosorption capacity as a function of biosorption time for the 12 different initial concentration values assayed. The biosorption curves were single, smooth and continuous leading to saturation of the biosorbent.

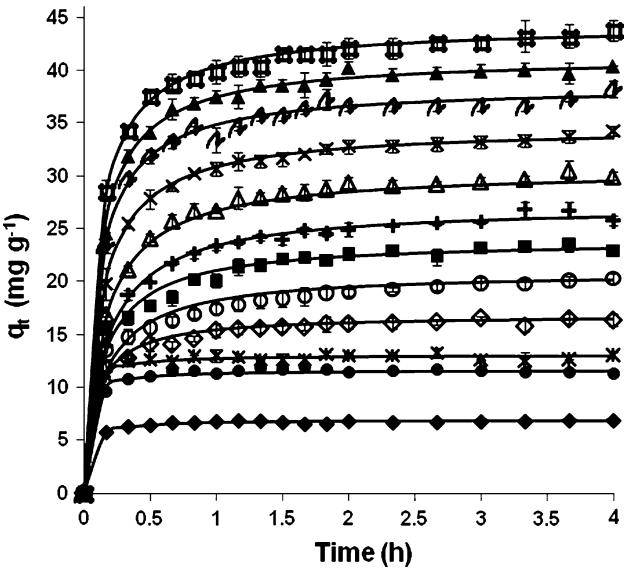

Fig. 2 Effect of initial metal concentration on Ni(II) biosorption by acetone-pretreated *R. glutinis* biomass. Initial Ni(II) concentration: *filled diamond* 10 mg l^{-1}; *filled circle* 20 mg l^{-1}; *Asterisk* 30 mg l^{-1}; *open diamond* 40 mg l^{-1}; *open circle* 60 mg l^{-1}; *filled square* 80 mg l^{-1}; *plus symbol* 100 mg l^{-1}; *open triangle* 130 mg l^{-1}; *multiplication symbol* 150 mg l^{-1}; *zig zag line* 200 mg l^{-1}; *filled triangle* 300 mg l^{-1}; *open square* 400 mg l^{-1}; *continuous line* pseudo-second-order model prediction. Conditions: solution pH = 7.5; temperature = 25°C; biosorbent concentration = 1 g l^{-1}. When not shown, *error bars* are smaller than symbol size

Biosorption capacity gradually increased as contact time increased, until it reached a maximum constant value. At this point, the Ni(II) amount adsorbed by the biosorbent

Table 2 Effect of initial Ni(II) concentration on the kinetic parameters of the pseudo-second-order model and equilibrium time

C_o (mg l^{-1})	Exp q_e (mg g^{-1})	t_e (h)	k_2 (g mg^{-1} h^{-1})	q_e (mg g^{-1})	r^2	SSE	RMSE
10	6.981	0.1667	3.669	6.96	0.9788	1.008	0.1865
20	11.382	0.333	3.021	11.7	0.9843	2.085	0.2681
30	12.741	0.5	2.814	13.14	0.9817	3.08	0.3259
40	17.099	1.167	0.6475	16.86	0.9892	3.143	0.3292
60	21.143	1.5	0.3243	20.94	0.9723	13.54	0.6832
80	23.438	1.667	0.3055	23.99	0.9759	15.3	0.7263
100	27.121	1.667	0.2275	27.14	0.9946	4.574	0.3971
130	30.563	1.833	0.2228	30.62	0.9985	1.59	0.2341
150	34.485	1.833	0.2368	34.57	0.9987	0.1601	0.2531
200	38.441	2.0	0.246	38.49	0.9968	4.899	0.4427
300	41.559	2.0	0.2375	41.35	0.9976	4.187	0.4092
400	44.447	2.0	0.2325	44.34	0.9956	8.922	0.5547

Conditions: Solution pH, 7.5; temperature, 25°C; shaking speed, 140 rpm; biosorbent concentration, 1 g l^{-1}

and the Ni(II) amount desorbed from the biosorbent showed a dynamic equilibrium. Statistical analysis revealed that the contact time needed to reach equilibrium depended on initial Ni(II) concentration (Table 2). At concentrations lower than 100 mg l^{-1}, equilibrium time (t_e) increased in parallel to initial metal concentration; in contrast, at concentrations above 150 mg l^{-1}, equilibrium time remained constant. Furthermore, equilibrium was reached in less than 30 min at low and in 2 h at very high initial Ni(II) concentrations (200–400 mg l^{-1}).

Biosorption capacity at equilibrium (exp q_e) increased from 6.98 to 44.45 mg g^{-1} as initial Ni(II) concentration rose from 10 to 400 mg l^{-1} (Table 2). This increase may be due to greater Ni(II) ion in solution available for biosorption. Besides, the increase in initial Ni(II) concentration could produce a stronger driving force [i.e., concentration gradient of Ni(II) ions] to overcome all mass transfer resistances of Ni(II) ions between the aqueous solution and the biosorbent, which results in a higher probability of collision between Ni(II) ions and the biosorbent. This, in turn, leads to a greater biosorption capacity of the metal ion [6]. These results also show that saturation of the biosorbent surface depends on initial Ni(II) concentration.

Table 2 also shows the parameters of the pseudo-second-order kinetic model (k_2 and q_e) obtained at the different initial Ni(II) concentrations assayed. For all concentration values, correlation coefficients for pseudo-second-order kinetics were within 0.972–0.999, and SSE as well as RMSE values were acceptable. Likewise, experimental q_e values (exp q_e) come very close to the values predicted by the pseudo-second-order model (Table 2). Furthermore, the pseudo-second-order kinetic model satisfactorily described the variations in Ni(II) biosorption capacity as a function of time (continuous lines in Fig. 2).

The rate constant (k_2) of the pseudo-second-order model decreased rapidly as initial metal concentration increased from 10 to 100 mg l^{-1}. At higher concentrations, k_2 remained virtually constant at a value of approximately 0.23 g mg^{-1} h^{-1} (Table 2). An explanation for this behavior is that, as initial metal concentration is increased, longer contact time is required to reach equilibrium (Fig. 2), as has been reported for different biosorption systems [2, 19, 36].

Studies in equilibrium: sorption isotherms

In the present study, the Ni(II) ion biosorption isotherm was generated by varying the initial concentration of the metal (10–400 mg l^{-1}), while the amount of biosorbent (1 g l^{-1}), the solution pH (7.5) and the temperature (25°C) were kept constant. The experimental biosorption isotherm is shown in Fig. 3. Several models of two (Langmuir, Freundlich, Dubinin-Radushkevich and Temkin), three (Sips, Radke-Prausnitz, Redlich-Peterson and Toth), and four (Fritz-Schluender) parameters were used to describe the experimental Ni(II) biosorption isotherm. The model parameters values along with 95% confidence intervals, as well as correlation coefficients (r^2), residue or SSE and RMSE values are shown in Table 3. In addition, data predicted by the isotherm models are shown in Fig. 3.

Among the two-parameter isotherm models, those by Langmuir and Freundlich showed the best fit to experimental Ni(II) sorption data. The Langmuir model has been used widely to estimate the maximum biosorption capacity whenever it was not possible to reach it experimentally, and contains the two most important parameters in a biosorption system, q_{max} and b [22]. The first (q_{max}) is attributed to the maximum capacity of sorption to complete saturation of the biosorbent, and the second (b) is a coefficient related to biosorbent-sorbate affinity. Experimental data reasonably fitted the Langmuir isotherm model, with a correlation coefficient (r^2) of 0.959 and acceptable SSE,

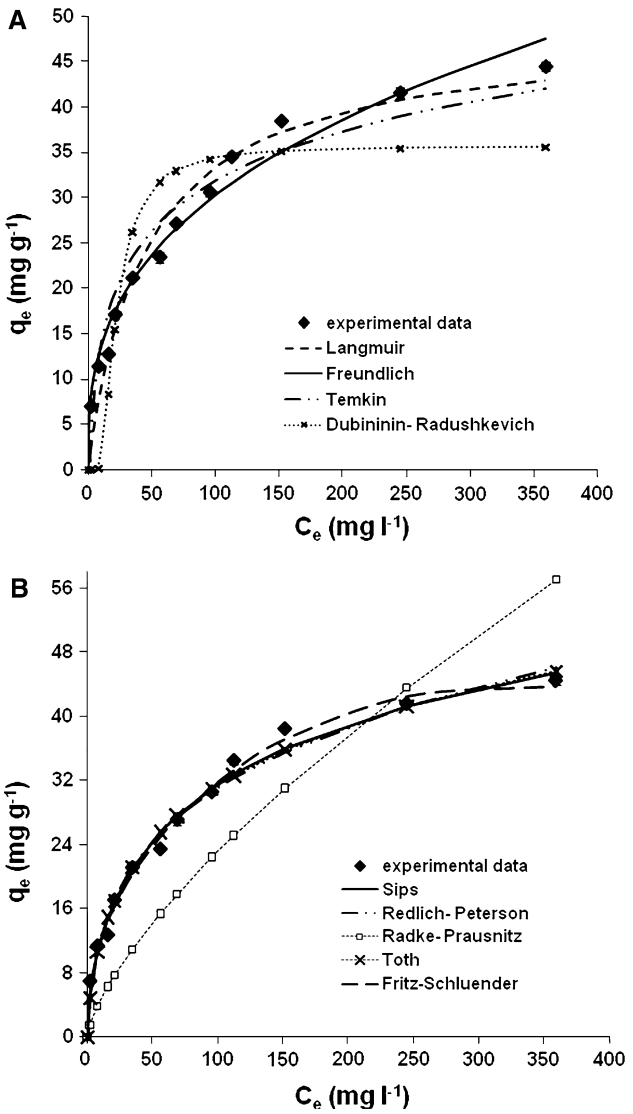

Fig. 3 Comparison between the experimental isotherm data and the calculated isotherm data derived from two-parameter (**a**), and three- and four-parameter (**b**) models for Ni(II) biosorption by acetone-pretreated *R. glutinis* biomass. Conditions: solution pH = 7.5; temperature = 25°C; biosorbent concentration = 1 g l^{-1}

RMSE and 95% confidence intervals values. The Langmuir model predicted a q_{max} of 48.28 mg g^{-1}, which approximates the experimental value of Ni(II) biosorption capacity at equilibrium (44.45 mg g^{-1}). The Freundlich isotherm model is suitable for describing multilayer adsorption on heterogeneous adsorbents [37]. The value for constant n in the Freundlich model was 2.831, which is within the interval of n values (n = 1–10), which indicate favorable biosorption [22].

The Temkin model did not adequately describe the Ni(II) sorption isotherm because the correlation coefficient value was low (r^2 = 0.934), both SSE and RMSE were higher than those obtained with the Langmuir and Freundlich

Table 3 Isotherm constants of two-, three-, and four-parameter models for Ni(II) biosorption onto acetone-pretreated *R. glutinis*

Two-parameter models		
Langmuir		
q_{max}	(mg g^{-1})	48.28 ± 5.9
B	(l mg^{-1})	0.022 ± 0.008
r^2		0.9591
SSE		68.54
RMSE		2.618
Freundlich		
k_F	(mg g^{-1})(mg l^{-1})$^{-1/n}$	5.945 ± 1.48
n		2.831 ± 0.402
r^2		0.9729
SSE		45.37
RMSE		2.13
Temkin		
a_T	(l mg^{-1})	0.5452 ± 0.3604
b_T	(J mol^{-1})	311.1 ± 58.2
r^2		0.9342
SSE		110.3
RMSE		3.321
Dubinin-Radushkevich		
q_{max}	(mg g^{-1})	35.65 ± 6.22
B_D	(mol^2 J^{-2})	6.24E-05 ± 5.2E-05
E	(J mol^{-1})	89.529
r^2		0.7269
SSE		457.800
RMSE		6.766
Three- and four-parameter models		
Sips		
$q$max	(mg g^{-1})	75.12 ± 38
b_s	(mg l^{-1})$^{-1/ns}$	0.04848 ± 0.015
n_s		1.704 ± 0.6
r^2		0.9859
SSE		23.59
RMSE		1.619
Radke-Prausnitz		
β_R		0.7052 ± 2.06
a_R	(l g^{-1})	1.07E + 04 ± 3.53E + 09
r_R	(l mg^{-1})	0.9006 ± 15.14
r^2		0.4912
SSE		853
RMSE		9.735
Redlich-Peterson		
β_{RP}		0.7382 ± 0.125
K_{RP}	(l g^{-1})	3.418 ± 4.14
a_{RP}	(mg l^{-1})$^{-\beta RP}$	0.3329 ± 0.63
r^2		0.9796
SSE		34.26
RMSE		1.951

Table 3 continued

Toth		
q_{max}	(mg g^{-1})	121.1 ± 171.05
b_T	(l mg^{-1})	0.09616 ± 0.198
n_T		3.307 ± 3.265
r^2		0.9836
SSE		27.45
RMSE		1.746
Fritz- Schluender (4-parameters)		
A_{FS}	(mg g^{-1})(mg l^{-1})$^{-\alpha FS}$	4.402 ± 0.314
α_{FS}		0.433 ± 0.0408
B_{FS}	(mg l^{-1})$^{-\beta FS}$	5.03E-07 ± 6.56E-08
β_{FS}		2.251 ± 0.2766
r^2		0.9925
SSE		12.58
RMSE		1.254

models and the 95% confidence interval for its parameters are large. Among the two-parameter models tested, the poorest fit to experimental values at equilibrium was obtained with the Dubinin-Radushkevich model, which presented the lowest correlation coefficient, very high SSE and RMSE values, wide 95% confidence intervals and predicted a q_{max} approximately 20% below the experimental value.

Considering the three-parameter isotherm models, with the exception of the Radke-Prausnitz model, all others fitted the experimental data of the Ni(II) sorption isotherm with higher correlation coefficient and lower SSE and RMSE than the two-parameter models. However, the confidence intervals of the three-parameter models were, in general, higher than those of the two-parameter models. Evidently, the Redlich-Peterson model was a good fit to the experimental data (Fig. 3), showing a high value for the correlation coefficient ($r^2 = 0.979$) and suitable SSE and RMSE values, but the 95% confidence interval for its parameters was very large. Similarly, although the Toth and Sips models rendered a high correlation coefficient value ($r^2 = 0.98$), low SSE and RMSE values, and described a tendency that was very close to that found within the studied concentration interval (Fig. 3), the predicted q_{max} values were 172.4% and 69% above the experimental result, respectively. Besides, the confidence intervals of the Sips and Toth models parameters were

Table 4 Comparison of Ni(II) biosorption capacities of some biosorbents

Biosorbent	T (°C)	pH	q (mg g^{-1})	Isotherm model	Reference
Bacteria					
Pseudomonas aeruginosa	37	NR	262.34E	Freundlich	[41]
Bacillus thuringiensis	25	6.0	22.5E	Langmuir, Freundlich	[1]
Escherichia coli BL21	28	NR	23.2E	Langmuir	[42]
Cyanobacteria					
Microcystis sp.	29	6.4	100.8E	Freundlich	[43]
Synechocystis sp.	25	4.5	30.3E	Freundlich	[44]
Lyngbya taylorii	RT	4.7	37.7P	Langmuir	[45]
Yeasts					
Candida lusitaniae 19	25	6.5	8.4E	NR	[17]
Candida guilliermondii 13	25	6.5	5.0E	NR	[17]
Saccharomyces cerevisiae	25	5	46.3P	Langmuir	[16]
Saccharomyces cerevisiae (protonated)	RT	6.75	11.4P	Langmuir	[2]
Rhodotorula glutinis	25	7.5	44.45E	Fritz- Schluender (4-parameters)	This work
Rhodotorula glutinis	70	7.5	63.53E		This work
Filamentous fungi					
Penicillium chrysogenum	30	5.5	45E	Langmuir	[46]
Aspergillus niger 405	25	5.0	14.1P	Langmuir	[47]
Rhizopus arrhizus	NR	7.5	18.7P	Langmuir	[48]
Phomopsis sp.	NR	6.0	6.0P	Langmuir	[49]
Polyporous versicolor	25	5.0	47P	Langmuir	[50]
Microalgae					
Scenedesmus obliquus	25	4.5	30.2P	Langmuir	[44]
Spirogyra insignis	NR	6.0	17.7P	Langmuir	[51]
Chlorella miniata	NR	7.4	1.37E	Langmuir	[52]

RT room temperature, *E* experimental data, *P* model prediction, *NR* not reported

wide. Taking into account the above results, the three-parameter models were not considered adequate to represent the data of Ni(II) biosorption at equilibrium.

The most satisfactory description of Ni(II) biosorption onto *R. glutinis* was provided by the Fritz-Schluender model. It rendered the highest correlation coefficient ($r^2 > 0.99$), the lowest SSE and RMSE values of the nine isotherm models tested here, and the confidence intervals of its parameters were very reasonable. The Fritz-Schluender model is empirical in nature and has a large number of constants. The increased number of constants would be able to simulate the model variations more accurately. In the case of biosorptive processes, the factors affecting sorption are many. So, in the absence of a theoretical model that could account for the chemical heterogeneity of the biosorbent surface, an isotherm model having a greater number of model constants would probably be able to predict better the biosorption isotherm [38]. In the present study, this is observed.

To the best of our knowledge, this is the first work to report the Fritz-Schluender model as the most adequate to represent biosorption of a heavy metal by the *Rhodotorula* species. The Langmuir isotherm has been used recurrently to analyze equilibrium biosorption data by *Rhodotorula* species, such as lead [13] and uranium biosorption [39] by *Rhodotorula glutinis*, and cadmium and lead biosorption by *Rhodotorula rubra* [40].

Table 4 shows the values of Ni(II) biosorption capacity of different microorganisms and the model used to describe biosorption at equilibrium. The Langmuir model is evidently acknowledged as the most adequate for most biosorption data. However, it must be mentioned that, in many cases, it was also the only one assayed, and finding that the correlation coefficient results were acceptable ($r^2 > 0.95$) no other models were assayed. Besides, it should be noted that several of the values for Ni(II) biosorption capacity shown on Table 4 are theoretical, i.e., they are capacity values predicted by the Langmuir model (data with superscript P), not necessarily reached experimentally.

The values for nickel biosorption capacity obtained in the present work were significantly higher than most results reported in the literature, with the exception of values for *Pseudomonas aeruginosa* and *Microcystis* sp. These results indicate that acetone-pretreated *R. glutinis* biomass is one of the best biosorbents hitherto reported for Ni(II) removal from aqueous solutions and could therefore be used effectively to detoxify wastewaters polluted with Ni(II).

Effect of temperature on Ni(II) biosorption

The present work examined the effect of temperature (25–70°C) on Ni(II) biosorption onto *R. glutinis*, at two different initial concentration values of the metal (60 and 150 mg l^{-1}). Figure 4 shows that at the two initial Ni(II) concentration values tested, the metal biosorption capacity onto *R. glutinis* increased as the temperature rose from 25°C to 70°C. This behavior indicates that the biosorption process is endothermic, i.e., it requires energy to be completed. At equilibrium, Ni(II) biosorption onto the *R. glutinis* biomass increased from 21.14 to 42.2 mg g^{-1} as the temperature rose from 25°C to 70°C at an initial concentration of 60 mg l^{-1}. At an initial concentration of

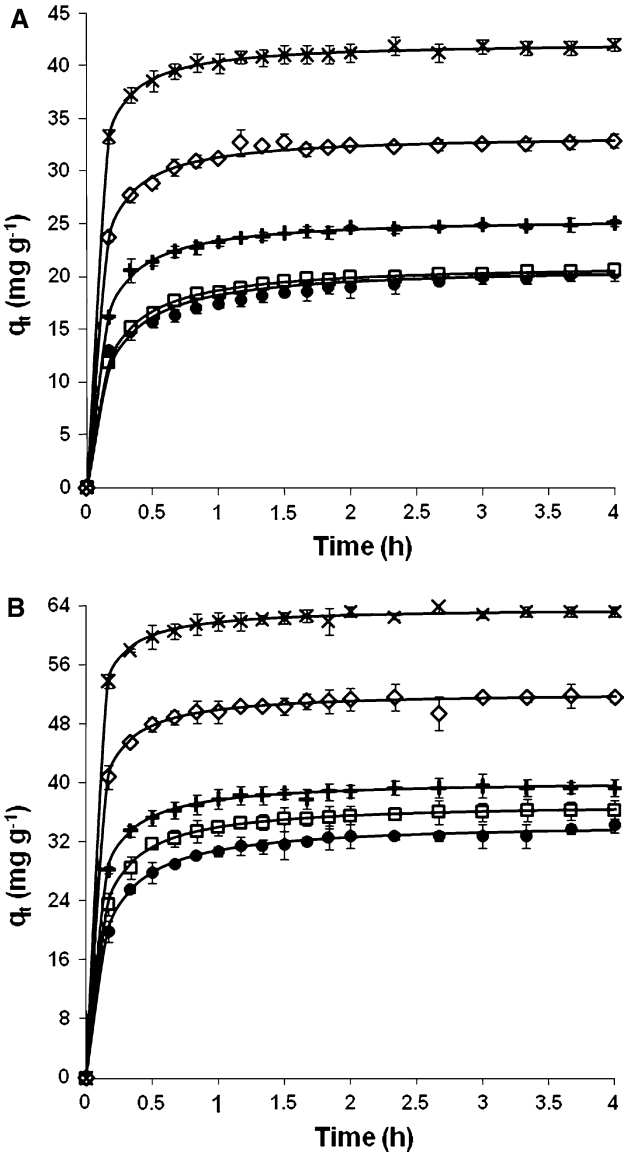

Fig. 4 Effect of temperature on Ni(II) biosorption by acetone-pretreated *R. glutinis* biomass. **a** Initial Ni(II) concentration = 60 mg l^{-1}; **b** initial Ni(II) concentration = 150 mg l^{-1}. Temperatures: *filled circle* 25°C; *open square* 35°C; + *symbol* 45°C; *open diamond* 60°C; *multiplication symbol* 70°C; *continuous line* pseudo-second-order model prediction. Conditions: solution pH = 7.5; biosorbent concentration = 1 g l^{-1}. When not shown, *error bars* are smaller than symbol size

Table 5 Effect of temperature on kinetic parameters of the pseudo-second-order model

T (°C)	Exp q_e [mg g^{-1}]	k_2 (g mg^{-1} h^{-1})	q_e (mg g^{-1})	r^2	SSE	RMSE
Initial Ni(II) concentration: 60 mg l^{-1}						
25	21.143	0.3242	20.94	0.9723	13.54	0.6832
35	21.240	0.3507	21.28	0.999	0.481	0.1288
45	25.630	0.4173	25.59	0.9987	0.8695	0.1732
60	33.460	0.4402	33.48	0.9972	3.146	0.3294
70	42.200	0.5262	42.25	0.9996	0.7682	0.1628
Initial Ni(II) concentration: 150 mg l^{-1}						
25	34.485	0.2368	34.57	0.9987	0.1601	0.2531
35	37.243	0.2781	37.28	0.9995	0.6875	0.154
45	40.360	0.3559	40.24	0.9982	2.954	0.3192
60	52.486	0.3995	52.35	0.9974	6.831	0.4853
70	63.531	0.5046	63.65	0.9989	4.352	0.3874

Conditions: Solution pH, 7.5; shaking speed, 140 rpm; biosorbent concentration, 1 g l^{-1}

150 mg l^{-1}, Ni(II) biosorption capacity increased from 34.48 to 63.53 mg g^{-1} (Table 5).

Increase in metal biosorption with rising temperature may be due to higher affinity of the metal binding sites, to an increment in the number of available active sites on the biosorbent surface, to the desolvation of the metal species, to the increase of diffusion rate of Ni(II) ions, and to the decrease in thickness of the boundary layer surrounding the biosorbent, such that the mass transfer resistance of metal ions in the boundary layer is reduced. Also, at higher temperatures, the energy of the system facilitates the binding of the metal ion to the biosorbent [6].

Figure 4 shows that the difference in Ni(II) biosorption capacity obtained at 25°C and 35°C is low, particularly at initial concentration of 60 mg l^{-1}. These results are in good agreement with those obtained by several authors, who have reported that the use of metabolically inactive cells as biosorbents shows almost no effect of temperature on metal adsorbance in the range of 25°C to 40°C [13, 30, 35].

Table 5 shows the kinetic parameters of the pseudo-second-order model for the five temperatures and two initial Ni(II) concentration levels tested in this work. Correlation coefficients were high ($0.972 < r^2 < 1.0$) and SSE and RMSE values low, which indicates the adequacy of the pseudo-second-order model to describe Ni(II) biosorption onto *R. glutinis* at the assayed temperatures and initial metal concentrations. The applicability of the pseudo-second-order kinetic model was verified by fitting the experimental data (continuous lines in Fig. 4). Results also show that the k_2 values increased as temperatures rose, confirming that the rate of biosorption is faster at higher temperatures, which is probably due to an increase in the interactions between Ni(II) ions and the biosorbent. This behavior is characteristic of endothermic reactions.

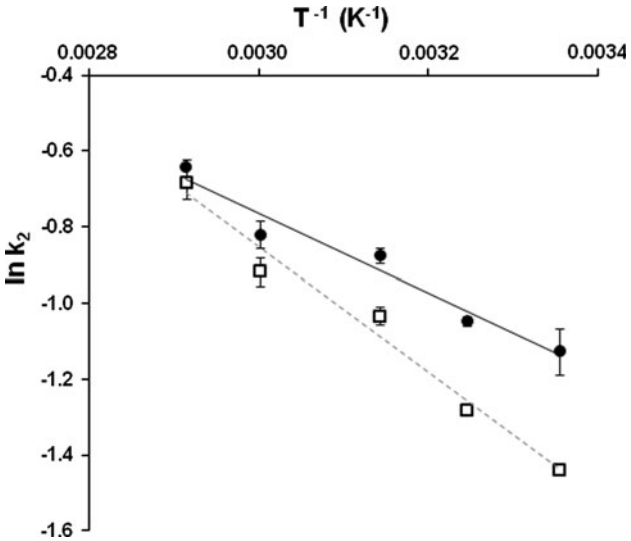

Fig. 5 Plot of ln k_2 versus T^{-1} for the biosorption of Ni(II) by acetone-pretreated *R. glutinis* biomass: *filled circle* initial Ni(II) concentration = 60 mg l^{-1}; *open square* initial Ni(II) concentration = 150 mg l^{-1}. Conditions: solution pH = 7.5; biosorbent concentration = 1 g l^{-1}. When not shown, *error bars* are smaller than symbol size

Previous studies have reported the endothermic nature of the heavy metal biosorption process, such as those of Cu(II) [53], Cr(III) [34], Cr(VI) [36], V(V) [54], Ni(II) [1, 6, 29, 50], Pb(II) [31], Zn(II) [55], and Cd(II) [56].

The effect of temperature on Ni(II) biosorption was examined in greater detail by applying the Arrhenius equation (Eq. 2). For the two initial Ni(II) concentrations assayed, the biosorption energy of activation (E_A) and frequency factor (A_0) were calculated from the slope and intercept of the straight lines obtained in the ln k_2 versus T^{-1} plots (Arrhenius plots), shown in Fig. 5. The E_A and A_0 values for the Ni(II) biosorption onto *R. glutinis* were

Table 6 Thermodynamic parameters for the biosorption of Ni(II) onto acetone-pretreated *R. glutinis*

T (°C)	$\Delta G^{\ddagger}$ (kJ mol^{-1})	E_A (kJ mol^{-1})	A_0 (g mg^{-1} h^{-1})	$\Delta S^{\ddagger}$ (kJ mol^{-1} K^{-1})	$\Delta H^{\ddagger}$ (kJ mol^{-1})
Initial Ni(II) concentration: 60 mg l^{-1}					
25	55.533				
35	57.192				
45	58.850	8.746	10.935	−0.166	6.088
60	61.338				
70	62.996				
Initial Ni(II) concentration: 150 mg l^{-1}					
25	56.278				
35	57.793				
45	59.309	13.751	60.947	−0.152	11.091
60	61.582				
70	63.098				

8.746 kJ mol^{-1} and 10.935 g mg^{-1} h^{-1} when the initial Ni(II) concentration was 60 mg l^{-1}, and 13.751 kJ mol^{-1} and 60.947 g mg^{-1} h^{-1} when the initial Ni(II) concentration was 150 mg l^{-1}, respectively (Table 6).

The magnitude of the activation energy provides a clue to the type of adsorption, which could be mainly physical or chemical. Activation energy for physical adsorption is usually not higher than 4.184 kJ mol^{-1}, and for chemical adsorption it ranges from 8.4 to 83.7 kJ mol^{-1} [24, 29]. Activation energy values found in the present work correspond to the chemical adsorption values. In conclusion, Ni(II) biosorption onto *R. glutinis* is an endothermic chemical adsorption process. In addition, the relatively low E_A values found herein indicate that the chemical biosorption process involves weak interactions between Ni(II) ions and the biosorbent, and that this biosorption has a low potential energy barrier [21].

The changes in biosorption entropy ($\Delta S^{\ddagger}$) and enthalpy ($\Delta H^{\ddagger}$) were calculated from the slope and the intercept of the straight line in the ln ($k_2\ T^{-1}$) versus T^{-1} plot (Fig. 6). In addition, the Gibbs free activation energy change ($\Delta G^{\ddagger}$) was calculated from the $\Delta S^{\ddagger}$ and $\Delta H^{\ddagger}$ values. Values for these thermodynamic parameters are shown in Table 6.

The values for $\Delta S^{\ddagger}$ and $\Delta H^{\ddagger}$ were −0.166 kJ mol^{-1} K^{-1} and 6.088 kJ mol^{-1} at initial Ni(II) concentration of 60 mg l^{-1}, and −0.152 kJ mol^{-1} K^{-1} and 11.091 kJ mol^{-1} for the 150 mg l^{-1} initial Ni(II) concentration. Values for $\Delta H^{\ddagger}$ were positive, which confirms that the reaction is endothermic and consequently consumes energy. The negative $\Delta S^{\ddagger}$ values indicate that the adsorption leads to order through the formation of an activated complex, suggesting that Ni(II) biosorption onto the *R. glutinis* surface is an associated mechanism [25]. Also, a negative $\Delta S^{\ddagger}$ value normally reflects that no significant change occurs in the internal structure of the biosorbent during the biosorption process [25, 57]. Negative $\Delta S^{\ddagger}$ values are not uncommon in metal adsorption [57].

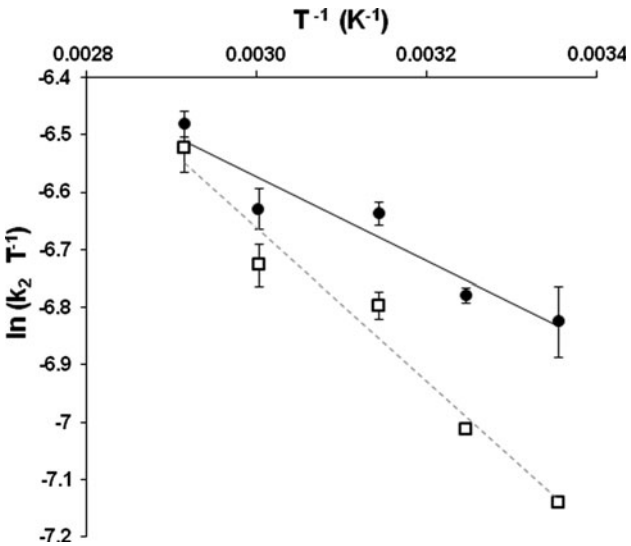

Fig. 6 Plot of ln ($k_2\ T^{-1}$) versus T^{-1} for the biosorption of Ni(II) by acetone-pretreated *R. glutinis* biomass: *filled circle* initial Ni(II) concentration = 60 mg l^{-1}; *open square* initial Ni(II) concentration = 150 mg l^{-1}. Conditions: solution pH = 7.5; biosorbent concentration = 1 g l^{-1}. When not shown, *error bars* are smaller than symbol size

The values for $\Delta G^{\ddagger}$ were positive at all assayed temperatures, suggesting the existence of an energy barrier for Ni(II) biosorption, that the biosorption reaction is endothermic and non-spontaneous, and confirming that an input of energy is required for the reactant molecules to have enough kinetic energy to overcome the energy barrier and the chemical reaction to take place [11, 25].

Conclusions

Acetone-pretreated *R. glutinis* cells exhibited higher Ni(II) biosorption capacity than untreated cells at pH values ranging from 3 to 7.5. This finding is interesting from a

commercial point of view because the acetone-pretreated *R. glutinis* biomass discarded as waste material from biotechnological processes could be used as a potential biosorbent to remove Ni(II) ions from aqueous solutions.

Biosorption of Ni(II) ions onto acetone-pretreated *R. glutinis* depended strongly on solution pH, initial Ni(II) concentration, shaking contact time and temperature. The Fritz-Schluender four-parameter model was the adsorption model best suited to describe the equilibrium data of Ni(II) biosorption. Results from the present kinetics and thermodynamic studies suggest that chemisorption may be the Ni(II) sorption mechanism. Acetone-pretreated *R. glutinis* exhibited a very high Ni(II) biosorption capacity (44.45 mg g^{-1}) at 25°C, and its capacity increased approximately 43% when a temperature of 70°C was used (63.53 mg g^{-1}). The high Ni(II) sorption capacity of acetone-pretreated *R. glutinis* places this biosorbent among the best adsorbents currently available to remove Ni(II) ions from industrial wastewaters.

References

1. Öztürk A (2007) Removal of nickel from aqueous solution by the bacterium *Bacillus thuringiensis*. J Hazard Mater 147:518–523
2. Padmavathy V, Vasudevan P, Dhingra SC (2003) Biosorption of nickel(II) ions on baker's yeast. Process Biochem 38:1389–1395
3. Pandey PK, Choubey S, Verma Y, Pandey M, Kalyan-Kamal SS, Chandrashekhar K (2007) Biosorptive removal of Ni(II) from wastewater and industrial effluent. Int J Environ Res Public Health 4:332–339
4. Subbaiah MV, Vijaya Y, Kumar NS, Reddy AS, Krishnaiah A (2009) Biosorption of nickel from aqueous solutions by *Acacia leucocephala* bark: kinetics and equilibrium studies. Colloid Surface B 74:260–265
5. Savolainen H (1996) Biochemical and clinical aspects of nickel toxicity. Rev Environ Health 11:167–173
6. Malkoc E (2006) Ni(II) removal from aqueous solutions using cone biomass of *Thuja orientalis*. J Hazard Mater B137:899–908
7. World Health Organization (WHO) (2005) Nickel in drinking-water. Background document for development of WHO guidelines for drinking-water quality. Geneva, World Health Organization (WHO/SDE/WSH/05.08/55)
8. Zafar MN, Nadeem R, Hanif MA (2007) Biosorption of nickel from protonated rice bran. J Hazard Mater 145:501–505
9. Ngwenya BT, Tourney J, Magennis M, Kapetas L, Olive V (2009) A surface complexation framework for predicting water purification through metal biosorption. Desalination 248:344–351
10. Volesky B (2003) Sorption and biosorption. Sorbex, Montreal
11. Wang J, Chen C (2009) Biosorbents for heavy metals removal and their future. Biotechnol Adv 27:195–226
12. Breierová E, Vajcziková I, Sasinková V, Stratilová E, Fišera M, Gregor T, Šajbidor J (2002) Biosorption of cadmium ions by different yeast species. Z Naturforch 57C:634–639
13. Cho DH, Kim EY (2003) Characterization of Pb^{2+} biosorption from aqueous solution by *Rhodotorula glutinis*. Bioprocess Biosyst Eng 25:271–277
14. Aksu Z, Eren AT (2007) Production of carotenoids by the isolated yeast of *Rhodotorula glutinis*. Biochem Eng J 35:107–113
15. Malisorn W, Suntornsuk C (2008) Optimization of β-carotene production by *Rhodotorula glutinis* DM28 in fermented radish brine. Bioresour Technol 99:2281–2287
16. Özer A, Özer D (2003) Comparative study of the biosorption of Pb(II), Ni(II) and Cr(VI) ions onto *S. cerevisiae*: determination of biosorption heats. J Hazard Mater B100:219–229
17. Kambe-Honjoh H, Sugawara A, Yoda K, Kitamoto K, Yamasaki M (1997) Isolation and characterization of nickel-accumulating yeasts. Appl Microbiol Biotechnol 48:373–378
18. Mitchell AM, Mellon MG (1945) Colorimetric determination of nickel with dimethylglyoxime. Ind Eng Chem Anal Ed 17:380–382
19. Ho YS, McKay G (1998) Sorption of dye from aqueous solution by peat. Chem Eng J 70:115–124
20. Febrianto J, Kosasih AN, Sunarso J, Ju YH, Indraswati N, Ismadju S (2009) Equilibrium and kinetic studies in adsorption of heavy metals using biosorbent: a summary of recent studies. J Hazard Mater 162:616–645
21. Cayllahua JEB, de Carvalho RJ, Torem ML (2009) Evaluation of equilibrium, kinetic and thermodynamic parameters for biosorption of nickel(II) ions onto bacteria strain, *Rhodococcus opacus*. Miner Eng 22:1318–1325
22. Basha S, Murthy ZVP (2007) Kinetic and equilibrium models for biosorption of Cr(VI) on chemically modified seaweed, *Cystoseira indica*. Process Biochem 42:1521–1529
23. Abdel-Salam M, Burk RC (2010) Thermodynamics and kinetic studies of pentachlorophenol adsorption from aqueous solutions by multi-walled carbon nanotubes. Water Air Soil Pollut 210:101–111
24. Sağ Y, Kutsal T (2000) Determination of the biosorption activation energies of heavy metal ions on *Zoogloea ramigera* and *Rhizopus arrhizus*. Process Biochem 35:801–807
25. Doğan M, Abak H, Alkan M (2009) Adsorption of methylene blue onto hazelnut shell: kinetics, mechanism and activation parameters. J Hazard Mater 164:172–181
26. Khambhaty Y, Mody K, Basha S, Jha B (2009) Kinetics, equilibrium and thermodynamic studies on biosorption of hexavalent chromium by dead fungal biomass of marine *Aspergillus niger*. Chem Eng J 145:489–495
27. Ewecharoen A, Thiravetyan P, Nakbanpote W (2008) Comparison of nickel adsorption from electroplating rinse water by coir pith and modified coir pith. Chem Eng J 137:181–188
28. Pümpel T, Macaskie LE, Finlay JA, Diels L, Tsezos M (2003) Nickel removal from nickel plating waste water using a biologically active moving-bed sand filter. Biometals 16:567–581
29. Aksu Z (2002) Determination of the equilibrium, kinetic and thermodynamic parameters of the batch biosorption of nickel(II) ions onto *Chlorella vulgaris*. Process Biochem 38:89–99
30. Ruiz MA (2000) Recuperación de metales pesados de soluciones diluidas por biosorción con bacteria. In: Medrano RH, Galan WL (eds) Biotecnología de Minerales. México, pp 235–262
31. Bulut Y, Tez Z (2007) Adsorption studies on ground shells of hazelnut and almond. J Hazard Mater 149:35–41
32. Al-Rub FAA, El-Naas MH, Benyahia F, Ashour I (2004) Biosorption of nickel on blank alginate beads, free and immobilized algal cells. Process Biochem 39:1767–1773
33. Baig KS, Doan HD, Wu J (2009) Multicomponent isotherms for biosorption of Ni^{2+} and Zn^{2+}. Desalination 249:429–439
34. Michalak I, Chojnacka K (2010) The new application of biosorption properties of *Enteromorpha prolifera*. Appl Biochem Biotechnol 160:1540–1556
35. Vilar VJP, Botelho CMS, Boaventura RAR (2005) Influence of pH, ionic strength and temperature on lead biosorption by *Gelidium* and agar extraction algal waste. Process Biochem 40:3267–3275
36. Tewari N, Vasudevan P, Guha BK (2005) Study on biosorption of Cr(VI) by *Mucor hiemalis*. Biochem Eng J 23:185–192

37. Oladoja NA, Asia IO, Aboluwoye CO, Oladimeji YB, Ashogbon AO (2008) Studies on the sorption of basic dye by rubber (*Hevea brasiliensis*) seed shell. Turkish J Eng Environ Sci 32:143–152
38. Basha S, Jha B (2008) Estimation of isotherm parameters for biosorption of Cd(II) and Pb(II) onto brown seaweed, *Lobophora variegata*. J Chem Eng 53:449–455
39. Bai J, Qin Z, Wang JF, Guo JS, Zhang LN, Fan FL, Lin MS, Ding HJ, Lei FA, Wu XL, Li XF (2009) Study on biosorption of uranium by *Rhodotorula glutinis*. Guang Pu Xue Yu Guang Pu Fen Xi/Spectrosc Spectral Anal 29:1218–1221
40. Salinas E, Elorza de Orellano M, Rezza I, Martinez L, Marchesvky E, Sanz de Tosetti M (2000) Removal of cadmium and lead from dilute aqueous solutions by *Rhodotorula rubra*. Bioresour Technol 72:107–112
41. Sar P, Kazy SK, Asthana RK, Singh SP (1999) Metal adsorption and desorption by lyophilized *Pseudomonas aeruginosa*. Int Biodeter Biodegrad 44:101–110
42. Kao WC, Huang CC, Chang JS (2008) Biosorption of nickel, chromium and zinc by MerP-expressing recombinant *Escherichia coli*. J Hazard Mater 158:100–106
43. Pradhan S, Singh S, Rai LC (2007) Characterization of various functional groups present in the capsule of *Microcystis* and study of their role in biosorption of Fe, Ni and Cr. Bioresour Technol 98:595–601
44. Çentikaya-Dönmez GC, Aksu Z, Öztürk A, Kutsal T (1999) A comparative study on heavy metal biosorption characteristics of some algae. Process Biochem 34:885–892
45. Klimmek S, Stan HJ, Wilke A, Bunke G, Buchholz R (2001) Comparative analysis of the biosorption of cadmium, lead, nickel, and zinc by algae. Environ Sci Technol 35:4283–4288
46. Deng S, Ting YP (2005) Characterization of PEI-modified biomass and biosorption of Cu(II), Pb(II) and Ni(II). Water Res 39:2167–2177
47. Filipović-Kovačević Ž, Sipos L, Briški F (2000) Biosorption of chromium, copper, nickel and zinc ions onto fungal pellets of *Aspergillus niger* 405 from aqueous solutions. Food Technol Biotechnol 38:211–216
48. Fourest E, Roux JC (1992) Heavy metal biosorption by fungal mycelial by-products: mechanisms and influence of pH. Appl Microbiol Biotechnol 37:399–403
49. Saiano F, Ciofalo M, Cacciola SO, Ramirez S (2005) Metal ion adsorption by *Phomopsis* sp. biomaterial in laboratory experiments and real wastewater treatments. Water Res 39:2273–2280
50. Dilek FB, Erbay A, Yetis U (2002) Ni(II) biosorption by *Polyporous versicolor*. Process Biochem 37:723–726
51. Romera E, Fraguela P, Ballester A, Blázquez ML, Muñoz JA, González F (2003) Biosorption equilibria with *Spirogyra insignis*. 15th international biohydrometallurgy symposium. IBS 2003. pp 783–792
52. Wong JPK, Wong YS, Tam NFY (2000) Nickel biosorption by two *chlorella* species, *C. vulgaris* (a commercial species) and *C. miniata* (a local isolate). Bioresour Technol 73:133–137
53. Pamukoglu MY, Kargi F (2007) Effects of operating parameters on kinetics of copper(II) ion biosorption onto pre-treated powdered waste sludge (PWS). Enzyme Microb Technol 42:76–82
54. Namasivayam C, Sangeetha D (2006) Removal and recovery of vanadium(V) by adsorption onto $ZnCl_2$ activated carbon: kinetics and isotherms. Adsorption 12:103–117
55. Babarinde NAA, Babalola JO, Adebisi OB (2008) Kinetic, isotherm and thermodynamic studies of the biosorption of zinc(II) from solution by maize wrapper. Int J Phys Sci 3:50–55
56. Kim T, Park S, Cho S, Kim H, Kang Y, Kim S, Kim S (2005) Adsorption of heavy metals by brewery biomass. Korean J Chem Eng 22:91–98
57. Mohan D, Singh KP, Singh VK (2005) Removal of hexavalent chromium from aqueous solution using low-cost activated carbons derived from agricultural waste materials and activated carbon fabric cloth. Ind Eng Chem Res 44:1027–1042